Food Chemistry: X 24 (2024) 102013

Contents lists available at ScienceDirect

Food Chemistry: X

journal homepage: www.sciencedirect.com/journal/food-chemistry-x

Effect of soluble dietary fiber from corn bran on pasting, retrogradation, and digestion characteristics of corn starch

Sheng Li, Yuqian Zheng, Zhilong Chen, Wenlong Xie, Liping Xiao, Dengji Gao, Jun Zhao *

College of Food Sciences and Engineering, Changchun University, Changchun 130022, China

ARTICLE INFO

Keywords:
Soluble dietary fiber
Corn starch
Processing properties

ABSTRACT

This study investigated the effect of twin-screw extruded-enzymatically prepared soluble dietary fibers (EESDF) on various properties of CS. Results showed that adding EESDF decreased the viscosity and crystallinity. Incorporating 10 % EESDF reduced the peak and final viscosities of CS by 323 cP and 380 cP, respectively. When stored for 14 d, EESDF reduced the relative crystallinity (RC) and enthalpy of retrogradation (ΔHr) of CS. The RC and the ΔHr were reduced by 4.83 % and 41.53 %, respectively, when adding 10 % EESDF. The resistant starch content was increased by 6.7 % when stored for 0 d with the addition of 10 % EESDF. The eGI value was decreased when adding 10 % EESDF. These findings showed that EESDF inhibited the retrogradation and digestion of CS. They will provide a basis for using EESDF as a quality control for starchy foods and for using starch in soft gels and foods for dysphagic categories.

1. Introduction

Starch is a naturally occurring macromolecular polysaccharide, mostly found in different plants' seeds and tubers. Its monomer is the α-D-glucose with the molecular formula ($C_6H_{10}O_5$) n. The monomeric glucose molecules are linked in different ways to form amylose and amylopectin through α-1,4 saccharide bonds and α-1,6 saccharide bonds. Native starches are frequently employed in food processing as thickeners, gelling agents, and fat replacements. However, native starches inherently have several limitations, such as poor mechanical properties, easy retrogradation, deterioration, and high glycemic index. These limitations have restricted the application of native starches in various fields, including the food industry.

Corn starch (CS) is the primary carbohydrate derived from corn bran. Due to its low cost and abundance, CS is a raw material for many industrial processes and a source of sustenance for people and animals. CS plays a vital role in the food industry because of its exceptional thickening, gelling, retention of water, and other practical properties. It is frequently used to improve the quality of dairy products, puddings, and other food items(Xu et al., 2024). However, many disadvantages of native CS, such as its tendency to retrograde and poor stability and water retention, have limited its application in processing and food production. In addition, starch-based foods generally have high glycemic index (GI) values. Consuming foods high in GI can increase blood glucose levels after meals. This increase is linked to an increased risk of metabolic disorders like diabetes, obesity, hyperlipidemia, and heart disease (Li & Ma, 2024). Therefore, it is necessary to modify the processing and digestion properties of starch to expand the applications of CS in food.

Hydrocolloids, or non-starch polysaccharides, enhance starch processing, digestion, and sensory qualities(Ji et al., 2023; Li et al., 2024). For the past few years, combining these materials with starch to enhance starch properties has emerged as a green and environmentally friendly modification technique(Ma et al., 2022). Adding Laminaria japonica polysaccharides to wheat starch(Zhou et al., 2022) and chitosan to corn-resistant starch(Liu et al., 2019) inhibited starch pasting. However, the incorporation of xanthan gum, linseed gum, and konjac gum raised the viscosity of corn-resistant starch(Liu et al., 2019). Moreover, the addition of soluble dietary fiber even remarkably improved the viscosity coefficient K and the storage modulus and loss modulus of starch.(Liu et al., 2019). In contrast, the acidic polysaccharide (glucuronoxylomannan) of silver ear mushroom decreased the storage modulus of potato starch(Pak et al., 2021). Xiao et al. (2020)found that the coolant polysaccharide extraction methods of sodium carbonate and cellulose affected the physicochemical characteristics of cassava starch. Cellulase-extracted polysaccharides inhibited starch pasting and decreased the setback value of starch, resulting in a remarkable decline in pasting viscosity and gel strength. The addition of sodium carbonate-extracted polysaccharides increased the pasting viscosity and gel hardness of

* Corresponding author.
E-mail address: zhaoj70@ccu.edu.cn (J. Zhao).

https://doi.org/10.1016/j.fochx.2024.102013
Received 12 August 2024; Received in revised form 28 October 2024; Accepted 14 November 2024
Available online 16 November 2024

starch and the setback value. In addition, the sodium carbonate-extracted polysaccharide promoted the generation of an ordered structure after starch pasting, causing an increase in viscosity and accelerating the short-term retrogradation of starch. At the same time, the cellulase-extracted polysaccharide inhibited the short-term retrogradation of starch by inhibiting the leaching of amylose. As mentioned above, the reports on the influences of hydrocolloids or non-starch polysaccharides on starch properties are inconclusive and somewhat contradictory. Moreover, studies on the effect of dietary fiber on the retrogradation properties and digestion properties of starch are more limited.

Therefore, we used the twin-screw extruded-enzymatically prepared soluble dietary fibers (EESDF)(Li et al., 2022), systematically investigated the effect of soluble dietary fibers on the gel properties of CS, including pasting, static rheological, and dynamic rheological properties. Furthermore, this study also investigated the relative crystallinity (RC), gel hardness, and moisture distribution of CS to determine the influence of EESDF on the long-term retrogradation of CS. Meanwhile, we evaluated the efficacy of soluble dietary fiber in inhibiting the digestion properties and reducing the glycemic index of CS, which was assessed by in vitro digestibility measurements. This study explores how soluble dietary fibers interact with CS, affecting its processing and digestion properties. The findings could provide a research foundation for better realizing the use of CS in soft gel foods and foods for people with dysphagia categories.

2. Materials and methods

2.1. Materials

Corn bran was purchased from Changchun Dacheng Biotechnology Development Co. Corn starch (CS) (product code: RT1152, 27.54 % amylose content, 15.41 % moisture content) was purchased from Shanghai RYON Biotechnology Co. (Shanghai, China). Twin-screw extruded-enzymatically prepared soluble dietary (EESDF) (Moisture: 7.34 ± 0.15 %, Protein: 9.62 ± 0.21 %, Fat: 4.28 ± 0.15 %, Ash: 2.39 ± 0.12 %, SDF: 76.07 ± 0.88 %) was obtained by using the method of Li et al. (2022). It was composed of mannose, galacturonic acid, glucose, xylose, and arabinose. Its average molecular weight is 4.00 × 10^3 Da. Heat-resistant α-amylase (A109182, 3400 U/mL) was bought from Aladdin Reagent (Shanghai, China). Alkaline protease (A10154, from *Bacillus licheniformis*, 200 U/mg) was purchased from Genye Biotechnology Co. (Guangzhou, China). Amyloglucosidase (A800618, from *Aspergillus niger*, 100,000 U/mL) was bought from McLean Biochemical Technology Co. (Shanghai, China). Analytical grade reagents and substances were used in this investigation in full.

2.2. Determination of pasting properties

The pasting properties of the starch systems were analyzed using a rapid viscosity analyzer (RVATECMASTER, Perten Instruments Ltd., Sweden). 3 g of CS was mixed with 0 %, 1 %, 2 %, 3 %, 5 %, and 10 % EESDF (*w*/w, dry starch-based) in RVA aluminum cylinders, and 25 mL of distilled water was added and stirred well. The samples were measured using the RVA Standard 1 method: stirring at 50 °C and 960 rpm (10 s), followed by heating from 50 °C to 95 °C (3.75 min) at a steady speed of 160 rpm, holding 95 °C for 2.5 min, cooling to 50 °C (3.75 min), and a final temperature hold of 50 °C for 2 min. Record peak viscosity, trough viscosity, breakdown viscosity, final viscosity, setback, peak time, and the sample's paste curve were acquired through the RVA program(Zhao et al., 2021).

2.3. Determination of rheological properties

The samples were equilibrated at 25 °C for 5 min after the RVA test. Static and dynamic rheological properties were determined using a rheometer (MCR302, Anton Paar, Austria) with stainless steel parallel plates (25 mm diameter). Silicone oil was applied to the borders of the parallel plates to stop water from evaporating during the measurement. Static shear flow behavior was measured using the following method. The gap was set to 1.0 mm, and the measurement temperature was controlled at 25 °C for all samples. Samples with constant flow properties were measured at shear rates from 0.1 s^{-1} to 300 s^{-1}. The variation of shear stress and viscosity with shear rate was recorded(Wu et al., 2013). The experimental data were fitted using a power law model:

$$\tau = k\gamma^n \quad (1)$$

where τ is shear stress (Pa), K is consistency coefficient (Pa·s^n), γ is shear rate (s^{-1}), and n is flow behavior index.

Dynamic viscoelastic properties tests were conducted using the method of Liu et al. (2021). Samples were measured at 25 °C with the gap fixed at 1.0 mm. The energy storage modulus (G') and loss modulus (G") were measured at oscillatory strains from 0.1 rad/s to 100 rad/s at 1 %. We performed all dynamic tests at 1 % strain because it was well within the linear viscoelastic range for all samples.

2.4. Determination of thermal properties

3 mg of corn starch was mixed with 0 %, 1 %, 2 %, 3 %, 5 %, and 10 % EESDF. The mixtures were transferred to an aluminum tray of a differential scanning calorimeter (DSC, Q2000, TA Instruments, USA) with 10 μL of ultrapure water. The mixtures were sealed with a lid and left at 25 °C for 12 h. The temperature was measured to increase from 30 °C to 120 °C at a 10 °C/min speed, and the thermal properties were determined. The proportion of the enthalpy of gelatinization (ΔHg) to the enthalpy of retrogradation (ΔHr) (ΔHr/ΔHg) was used to visualize the retrogradation rate (R%).

2.5. Determination of Fourier transform infrared spectroscopy

FT-IR analysis was performed according to the method of Zhou et al. (2019). Starch-soluble dietary fiber gels obtained by the RVA procedure and starch gels retrograded at 4 °C for 14 days were freeze-dried, grounded, and mixed with dried KBr powder, respectively. The mixed powders were grounded again and pressed under pressure at 15 MPa for 1 min. Fourier transform infrared spectroscopy (VERTEX 70, Bruker, Germany) was used to measure the IR spectra of each sample. The spectra were measured over the range of 4000 cm^{-1} to 400 cm^{-1} with a resolution of 4 cm^{-1} and 64 scans. The spectra were analyzed using OMINIC software.

2.6. Low-field nuclear magnetic resonance (LF-NMR)

The starch gel for RVA measurements was weighed 1 g in a low-field NMR sample tube. The low-field NMR analyzer (MesoMR23, Shanghai Neumay Electronic Technology Co., Ltd., China) was used to evaluate the Transverse relaxation time (T_2) at 35 °C under the Carr-Purcell-Meiboom-Gill (CPMG) sequence. The Multi Exp Inv analysis software was used to examine the T_2 data (Xie et al., 2020).

2.7. Determination of gel hardness

The approach of Zhong et al. (2020) was used to determine the textural properties. RVA samples were kept at 4 °C for 24 h, and gel hardness was measured using a texture analyzer (TA-XT, Stable Micro System, UK). All samples were measured with a cylindrical probe (P 0.5). The gels were compressed with a trigger force of 5 g at a test rate of 1 mm/s, and the test distance was set to 10 mm. Each gel is cylindrical with a diameter of 36 mm and a height of 40 mm.

2.8. Determination of X-ray diffraction (XRD)

Gel samples kept at 4 °C for 0 d and 14 d were freeze-dried and measured with an X-ray diffractometer (D8 Advance, Bruker, Germany) at 40 kV voltage, 40 mA current. Scanning angles ranged from 5° to 40° (2θ), and the scanning frequency was 3°/min. All sample diffraction spectra were analyzed using Jade 6.0 software.

2.9. Determination of in vitro digestion of starch

The in vitro digestion of starch was determined by measuring the starch based on the approach of Englyst et al. (1992). The samples (CS-EESDF mixtures) were first pasted at 95 °C, then cooled to room temperature, and then simulated at 37 °C for digestion. A sample that was accurately weighed at 0.5 g was added to 10 mL of acetate buffer (0.1 M, pH 5.2) with 6 glass beads (to simulate gastrointestinal motility). The mixtures were shaken well and watered at 37 °C for 10 min. Add 2.5 mL of enzyme digest and digest at 37 °C with shaking. The reaction solution (0.5 mL) was removed at 0, 20, 40, 60, 90, and 120 min to inactivate the enzyme by adding 20 mL of ethanol at a concentration of 66 %. Then centrifuged at 5000 r/min for 5 min. The supernatant (0.1 mL) was added to 3 mL of GOPOD (glucose kit solution) and reacted at 45 °C for 20 min. By analyzing glucose measurements and hydrolysis rates, respectively, we determined the amount of Rapidly digestible starch (RDS), slowly digestible starch (SDS), and resistant starch (RS) with the following equations:

$$RDS(\%) = (G_{20} - G_0)/TS \times 0.9 \times 100 \quad (2)$$

$$SDS(\%) = (G_{120} - G_{20})/TS \times 0.9 \times 100 \quad (3)$$

$$RS(\%) = 100 - RDS(\%) - SDS(\%) \quad (4)$$

G_0, G_{20}, and G_{120} (mg) in the formula represent the glucose content released at 0 min, 20 min, and 120 min, respectively, and TS (mg) represents the total starch content.

2.10. Starch hydrolysis dynamics and prediction of the glycemic index

The digestion hydrolysis dynamics of starch were obtained by substituting the digestion data into a first-order kinetic model based on the method of Lu et al. (2022). The first-order equation is as follows:

$$C_t = C\infty\left(1 - e^{-kt}\right) \quad (5)$$

C_t is the amount of starch digested at time t (min), C_∞ is the estimated amount of starch digested at the final time, k (min^{-1}) is the first-order kinetic coefficient, and *t* is the digestion time.

The integral area of the hydrolysis curve about the X-axis was measured according to the dynamic equation. The hydrolysis index HI was the ratio of the integral area of the sample to that of the standard sample (white bread). The estimated glycemic index eGI (Ye et al., 2018) was evaluated and determined using the following equation:

$$eGI = 39.71 + 0.549HI \quad (6)$$

2.11. Statistical analysis of the data

Every experiment was run three times, with the findings expressed as mean ± SD and examined using SPSS 25.0 (SPSS Inc., Chicago, IL, USA). Each image and graph were described by Origin 2018 software (Stat-Ease Inc., Minneapolis, MN, USA) and evaluated by Jade 6.0 software (Materials Data, Inc., USA). Differences between samples were compared using ANOVA with Tukey post hoc test. It was deemed statistically significant when $p < 0.05$.

3. Results and discussions

3.1. Effect of EESDF on pasting properties of CS

Starch pasting is the expansion of starch granules at a certain temperature, breaking the hydrogen bonds of starch granules in the crystalline and amorphous regions. The pasting curves of CS with 1 %, 2 %, 3 %, 5 %, and 10 % EESDF are shown in Fig. 1, and the pasting parameters are shown in Table 2. The starch granules with various concentrations of EESDF absorbed water and swelled, and the paste viscosity increased markedly after 200 s. When the temperature reached 95 °C, the ordered structure of the internal crystalline area of starch was destroyed and transformed into a disordered structure. Meanwhile, the starch granules ruptured and formed a paste with viscosity. Finally, the starch molecules were entangled with the decrease in temperature to create a starch gel with a network structure. The modification of soluble dietary fiber has been demonstrated to affect the pasting properties of CS. Consequently, the pasting curve was altered. Upon reaching 5 % and 10 % EESDF additions, the CS pasting curves exhibited a notable downward shift.

Table 2 displays the pasting characteristics of CS at varying EESDF concentrations (1 %, 2 %, 3 %, 5 %, and 10 %). The addition of EESDF higher than 2 % markedly decreased the peak viscosity (PV), breakdown (BD) value, setback (SB) value, and final viscosity (FV) of CS. In contrast, the peak time and the pasting temperature were increased when 10 % EESDF was added. Meanwhile, there were no significant differences in the changes of through viscosity (TV). When 10 % EESDF was added, the PV of CS was reduced from 2810 ± 28 cP to 2487.33 ± 4.04 cP, and the FV was reduced from 2709.67 ± 44.38 cP to 2329 ± 6.93 cP. This phenomenon demonstrated that EESDF restricted the swelling of CS, thus reducing the viscosity. (Ye et al., 2018) The reduction of FV may be because EESDF limited the swelling of CS granules and the leaching of amylose by adhering to the surface of the CS granules. Consequently, throughout the pasting process, there was less leaching and frictional action of the internal components. Non-starch polysaccharides have a notable amount of hydrophilic groups, which could compete with the water available in the amorphous region of the starch molecule. This ability could reduce the water available in the amorphous area of the starch molecule, resulting in the amorphous area of the starch molecule not being able to obtain sufficient water at the beginning of the pasting and delaying the pasting of the starch(Tester & Sommerville, 2003). Furthermore, incorporating 10 % EESDF increased the pasting temperature from 79.32 ± 0.46 °C to 79.93 ± 0.03 °C and the pasting time from 5.24 ± 0.04 min to 5.33 ± 0 min. The upsurge in the pasting temperature and the pasting time also proved that the EESDF hindered the pasting of starch. The BD value refers to the difference between the PV

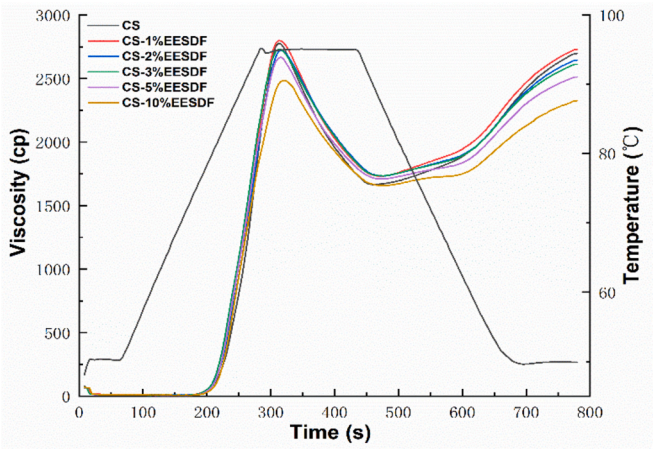

Fig. 1. Pasting curves of corn starch with various additions of EESDF determined by RVA.

and the TV. It displays starch granules' integrity, stability, and shear resistance and indicates the extent of stability and disruption of starch granules throughout the pasting process.(Tester & Sommerville, 2003) The BD value decreased with the addition of EESDF and the more EESDF added, the more decreased. This decrease indicated that EESDF enhanced the stability of CS. Moreover, incorporating EESDF resulted in a lower SB value of CS. The SB value predicts the retrogradation of the viscosity of CS during cooling. 2 % EESDF remarkably reduced the SB value of starch from 1011 ± 17.44 cp to 928.67 ± 16.17 cp. The SB value of starch added with 5 % and 10 % EESDF decreased by 19.55 % and 34.22 %, respectively, with the increase in the amount of EESDF added. This finding showed that EESDF inhibited the short-term retrogradation of starch and hindered the rearrangement of ordered structures during the cooling process of starch molecules. This may be because the interaction between the leached amylose and the EESDF interferes with the interaction between the amylose and the amylose through hydrogen bonding interactions.

3.2. Effect of EESDF on rheological properties of CS

3.2.1. Static rheological properties

The rheological characteristics of the CS paste samples with various EESDF concentrations were shown in Fig. 2 (A, B). All the samples exhibited notable shear thinning behavior. The starch pastes without EESDF addition presented the highest shear stress and viscosity as the shear rate increased. The decrease in starch viscosity and the addition of EESDF showed a dependency trend. Increasing the amount of EESDF added dramatically reduced the viscosity of the starch paste, which coincided with the results found in the RVA test.

All the parameters after fitting the power-law model are represented in Table 1. All samples had a flow behavior index (n) markedly less than 1, suggesting that the starch paste is a non-Newtonian fluid with pseudoplastic properties(Liu et al., 2021). The decrease in n values with the addition of EESDF revealed an improvement in the pseudo-plasticity of the starch paste. These results could be explained by the network structures that formed in the starch paste and EESDF to produce a notable increase in shear resistance. The increase in the pseudo-plasticity of starch suggests an excellent potential for its application in foods for people with dysphagia. The fitted R^2 of the upward and downward curves were in the range of 98.1 %–99.0 % interval, indicating that the power-law model can be used to describe the change in flow behavior. The consistency coefficient of starch (the K value) is used as a standard of viscosity.(Joshi et al., 2014) The incorporation of 1 % EESDF diminished the K value from 246.61 ± 12.72 (upward curve),78.03 ± 3.70 (downward curve) to 214.09 ± 26.26 (upward curve), 70.40 ± 3.26 (downward curve). The decrease in K values showed that the small quantity of EESDF addition could decrease starch viscosity. The K values diminished with the rise of EESDF additions. The reduction in K value was most pronounced in all samples with the addition of 10 % EESDF. The upward curve consistency factor was reduced to 156.54 ± 19.11, while the downward curve consistency factor was reduced to 52.51 ± 2.39. According to the study of Lei et al. (2020), the decrease in intermolecular flow resistance due to the low percentage of long amylose could explain the decrease in the K value. The low percentage of amylose might be related to the interaction of added EESDF with leached amylose through hydrogen bonding. We can obtain the area of the hysteretic loop by calculating the difference between the area of the upward and downward curves and the X-axis. The size of the hysteretic loop represents the amount of work needed to destroy the gel network structure. The small hysteretic loop represents the starch's strong shear resistance and small hysteresis. The starch paste easily resists the external force and is easier to recover to its original

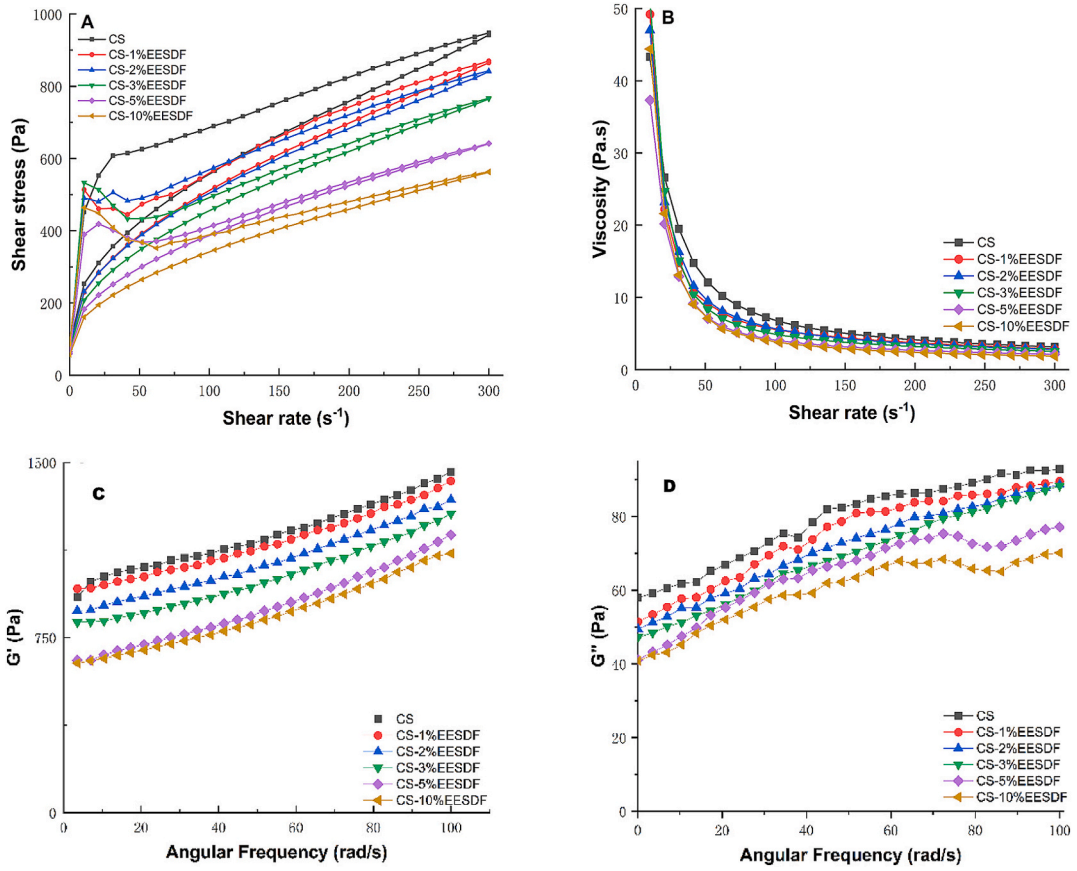

Fig. 2. Flow properties (A) and viscosity properties (B) of corn starch paste with different additions of EESDF. Storage modulus G' (C) and loss modulus G" (D) of corn starch with different additions of EESDF.

Table 1
Flow behavior of CS with various additions of EESDF.

Samples	up			down			hysteretic loop(Pa.s^{-1})
	K(Pa.s^n)	n	R^2	K(Pa.s^n)	n	R^2	
CS	246.61 ± 12.72^a	0.23 ± 0.01^b	0.981	78.03 ± 3.70^a	0.43 ± 0.01^a	0.989	31,349
CS-1 %EESDF	214.09 ± 26.26^{ab}	0.28 ± 0.02^a	0.985	70.40 ± 3.26^{bc}	0.43 ± 0.01^a	0.990	19,416
CS-2 %EESDF	192.89 ± 26.00^{bc}	0.24 ± 0.02^b	0.985	73.94 ± 3.31^{ab}	0.42 ± 0.01^a	0.989	17,199
CS-3 %EESDF	193.92 ± 17.29^{bc}	0.23 ± 0.03^b	0.982	64.64 ± 2.99^{cd}	0.43 ± 0.01^a	0.990	17,730
CS-5 %EESDF	161.52 ± 18.02^c	0.23 ± 0.02^b	0.981	58.83 ± 2.74^d	0.41 ± 0.01^a	0.990	16,016
CS-10 %EESDF	156.54 ± 19.11^c	0.15 ± 0.02^c	0.985	52.51 ± 2.39^e	0.41 ± 0.01^a	0.989	11,054

Note: Results are expressed as mean ± standard deviation ($n = 3$), and values with different letters in the same column differ significantly ($p < 0.05$).

state. It is not easy to recover to the original state after the external force destroys the structure, which indicates that the starch has poor shear resistance(Wang et al., 2022). The size of the hysteretic loop decreased with the addition of EESDF, indicating a lower hysteresis, suggesting that EESDF improved the starch's resistance to shear. This result is consistent with the BD value in the RVA observations.

3.2.2. Dynamic rheological properties

Elasticity and viscosity of starch gels are important indicators of starch processing and can anticipate alterations in textural properties during starch food processing. The dynamic rheological parameters energy storage modulus (G') and loss modulus (G") are related to the solid elastic and liquid viscous properties, respectively. The changes of G' and G" can be visualized as changes in the elasticity and viscosity of the starch gels. The G' value in Fig. 2 (C) remarkably exceeded the G" in Fig. 2 (D), showing the predominance of elasticity of starch in the viscoelastic behavior among the samples. Moreover, the two moduli of all samples did not cross each other, revealing a linear viscoelastic region. The G' and G" values rose with the increasing angular frequency, showing a high-frequency dependence, which indicated a strong correlation between EESDF and CS in the integrated system. The same phenomenon was also found in the study by Wang et al. (2021). All these findings above demonstrated that all samples showed a typical gel state. EESDF incorporation remarkably influenced the viscosity and elasticity of starch gels. Increasing the incorporation of EESDF resulted in weaker elasticity of the gels. EESDF inhibited the short-term retrogradation of starch, according to the RVA findings. When increasing the addition of EESDF, the short-term retrogradation of starch was markedly inhibited, as was the recrystallization of starch to generate an ordered structure. These inhibitions produced a softening of the starch gel, leading to less elasticity. This reduced the elasticity of the amylose gels by interfering with the starch interactions, delaying the aggregation and formation of an ordered structure among the starch. As a non-starch polysaccharide, EESDF has a large number of hydrophilic groups inside, which compete with the amorphous region of CS for water, limiting the swelling of CS. This limitation decreased the viscosity of CS.

3.3. Effect of EESDF on thermal properties of CS

The DSC determined thermal properties of the pasted and retrograded gels of CS with EESDF were displayed in Table 2. Overall, the paste onset temperatures (T_o) and peak temperatures (T_p) of the starches increased, and the enthalpy of gelatinization(ΔHg) values declined with the increase of EESDF addition. This finding was similar to the study of Luo et al. (2017). During the pasting process of CS, with the incorporation of EESDF, the T_o of CS also increased. When 5 % and 10 % EESDF were added, the T_o of CS increased by 2.28 °C and 3.52 °C, respectively. The rise in pasting temperature is linked to the hydrophilic properties of hydrocolloids. Hydrocolloids have good hydrophilicity and water-holding properties. They can also absorb water on the surface of starch molecules to form a material barrier, slowing water entry into the starch granules. Thus, they can delay the water-absorbing expansion of starch in amorphous areas. Meanwhile, the existence of hydrocolloids also reduced the water availability of starch molecules, decreased the flowability of water as a heat transfer medium, and delayed the pasting of starch. All these functions led to a lag in the pasting process. The T_p of the starch increased with the increase of EESDF addition. The T_p increased from 70.19 °C to 73.78 °C when 10 % EESDF was added. This consequence also corresponded to the above speculation, proving that EESDF delayed the pasting process of CS.

The ΔHg is the thermal energy required for starch gelatinization, reflecting the difficulty of achieving gelatinization. It is thought to be related to the double helix and crystalline order, and its decrease indicates a weakened double helix and crystalline-ordered structure. We found lower ΔHg of the starch by adding EESDF than the ΔHg of native CS (11.98 J/g). The changes between the ΔHg of small amounts (1 % and 2 %) of EESDF added were not evident. The ΔHg of starch with 3 %, 5 %, and 10 % EESDF added decreased by 1.09 J/g, 1.74 J/g, and 2.80 J/g, respectively. These findings suggested, to a certain extent, that the incorporation of EESDF declined the energy required to transform starch from the suspension state to the gelatinized state. And the effect became more obvious as the quantity of addition increased. Hydrocolloids have been shown to reduce the ΔHg by restricting the water flow and content in the system(Qiu et al., 2015). In addition, modified soluble dietary fibers have relatively small molecular weights. Small molecular polysaccharides can more easily enter the molecular interior of starch and interfere with the formation of the double helix and crystallization of the starch molecule, thus affecting starch gelatinization.

The enthalpy of retrogradation (ΔHr) represents the degree of recrystallization during starch retrogradation in which the starch recrystallizes into an ordered structure. The retrogradation rate R is expressed as the ratio of the enthalpy of gelatinization (ΔHg) to the enthalpy of retrogradation (ΔHr) (ΔHr/ΔHg). They are often used to indicate the degree of retrogradation of starch gels. The ΔHg of CS was obviously higher than the. ΔHr. The retrogradation process of starch is a thermally reversible recrystallization process divided into nucleus formation, nucleus propagation, and nucleus maturation processes. In this experiment, the ΔHr primarily represents the degree of amylose retrogradation. The retrogradation of amylose requires higher thermal energy to return to the original crystal state, while amylopectin can return to the crystal state below 120 °C(Qiu et al., 2015). In addition, the pasting and peak temperatures of starch gels reduced remarkably after 14 days of retrogradation. This phenomenon is related to the formation of unstable nuclei during the recrystallization of amylopectin. The ΔHr was reduced by 25.34 % and 41.53 % with the addition of 5 % and 10 % EESDF, respectively. The R-value declined from 55.68 % to 53.69 % when 1 %EESDF was added, and the R-value decreased with the increase in the incorporation of EESDF. These reductions demonstrated that adding EESDF could dramatically decrease the retrogradation and retard the recrystallization of CS.

The inhibitory influence of dietary fibers on the degree of CS retrogradation and recrystallization is because of the hydrogen-bounding interactions between CS and water or dietary fibers. Furthermore, dietary fibers have a polyhydroxy structure, which tends to interfere with the development of hydrogen bonding between water and starch molecules through hydrogen bonding(Tian et al., 2009). Dietary fibers

Table 2
Pasting properties and thermal properties of CS-EESDF systems.

Samples	Peak Viscosity (cP)	Trough Viscosity (cP)	Break Down (cP)	Final Viscosity (cP)	Setback (cP)	Peak Time (min)	Pasting Temp (°C)	Gelatinization				Retrogradation				R(%)
								T_0 (°C)	T_p (°C)	T_c (°C)	ΔHg (J/g)	T_{0r} (°C)	T_{pr} (°C)	T_{cr} (°C)	ΔHr (J/g)	
CS	2810 ± 28^{a}	1698.67 ± 53.15^{ab}	1111.33 ± 49.00^{a}	2709.67 ± 44.38^{a}	1011 ± 17.44^{a}	5.24 ± 0.04^{b}	79.32 ± 0.46^{b}	66.31 ± 0.02^{f}	70.19 ± 0.08^{e}	80.81 ± 0.59^{a}	11.98 ± 0.24^{a}	41.93 ± 1.43^{d}	56.03 ± 0.63^{a}	74.59 ± 3.19^{a}	6.67 ± 0.01^{a}	55.68 ± 0.01^{a}
CS-1 % EESDF	2782.67 ± 26.56^{a}	1719.67 ± 23.09^{ab}	1063 ± 3.46^{b}	2711.33 ± 30.60^{a}	991.67 ± 7.51^{a}	5.22 ± 0.04^{b}	79.1 ± 0^{b}	66.97 ± 0.10^{e}	70.96 ± 0.27^{d}	80.40 ± 0.65^{ab}	11.72 ± 0.13^{b}	42.61 ± 0.24^{cd}	55.93 ± 0.01^{a}	76.01 ± 1.67^{a}	6.29 ± 0.01^{b}	53.69 ± 0.01^{a}
CS-2 % EESDF	2712 ± 10.39^{bc}	1726.67 ± 23.67^{ab}	1005.33 ± 13.28^{c}	2635.33 ± 7.51^{b}	928.67 ± 16.17^{b}	5.27 ± 0^{b}	79.23 ± 0.12^{b}	67.39 ± 0.12^{d}	71.21 ± 0.21^{d}	79.96 ± 0.29^{ab}	11.72 ± 0.01^{b}	43.64 ± 0.39^{bc}	56.32 ± 0.34^{a}	76.58 ± 1.72^{a}	6.22 ± 0.04^{b}	53.04 ± 0^{a}
CS-3 % EESDF	2727.33 ± 2.31^{b}	1722.67 ± 9.81^{a}	1004.67 ± 7.51^{c}	2615.33 ± 2.89^{b}	892.67 ± 12.70^{c}	5.24 ± 0.04^{b}	79.23 ± 0.14^{b}	67.79 ± 0.08^{c}	71.89 ± 0.30^{c}	79.68 ± 0.41^{b}	10.89 ± 0.02^{c}	44.23 ± 0.13^{b}	56.26 ± 0.53^{a}	75.22 ± 1.08^{a}	5.42 ± 0.22^{c}	49.76 ± 0.02^{b}
CS-5 % EESDF	2677.67 ± 13.28^{c}	1707.67 ± 4.04^{ab}	970 ± 17.32^{c}	2521 ± 17.32^{c}	813.33 ± 21.36^{d}	5.24 ± 0.04^{b}	79.17 ± 0.12^{b}	68.59 ± 0.01^{b}	72.44 ± 0.20^{b}	80.33 ± 0.01^{ab}	10.24 ± 0.10^{d}	44.62 ± 0.29^{ab}	56.60 ± 0.27^{a}	76.49 ± 0.39^{a}	4.98 ± 0.12^{d}	48.59 ± 0.01^{b}
CS-10 % EESDF	2487.33 ± 4.04^{d}	1664 ± 12.12^{b}	823.33 ± 8.08^{d}	2329 ± 6.93^{d}	665 ± 5.20^{e}	5.33 ± 0^{a}	79.93 ± 0.03^{a}	69.83 ± 0.04^{a}	73.78 ± 0.02^{a}	79.99 ± 0.06^{ab}	9.18 ± 0.03^{e}	45.75 ± 0.38^{a}	56.57 ± 0.28^{a}	75.59 ± 0.69^{a}	3.90 ± 0.15^{e}	42.46 ± 0.02^{c}

Note: T_0 denotes the starting temperature; T_p denotes the peak temperature; T_C denotes the ending temperature; ΔH denotes enthalpy. Results are expressed as mean ± standard deviation ($n = 3$), and different letters in the same column indicate significant differences ($p < 0.05$).

compete to form hydrogen bonds between water molecules, making less water and hydrogen bonds available to starch molecules. This inhibits the formation of hydrogen bonds between starch molecules and inhibits the recrystallization of starch molecules during storage, as well as short-term and long-term retrogradation during storage.

3.4. Effect of EESDF on CS Fourier transform infrared spectroscopy

We use the Fourier transform infrared spectroscopy to measure the changes in various chemical bonds during the storage of samples. These changes reflect information such as conformational shifts and the helical structure of starch. Fig. S1 shows the infrared spectra of the starch gels. After incorporating EESDF, the infrared spectra showed no additional absorption peaks. This indicated that new chemical bonds were not created between starch and EESDF, and the main force between starch and EESDF was hydrogen bonding(Tian et al., 2009).

We could obtain the absorption peaks and intensities after the deconvolution of the IR spectra by OMNIC software in Fig. S1 (C, D). The IR spectra between 1200 cm^{-1} and 800 cm^{-1} exhibit variations in the short-range ordered structure of starch, as the spectra in this range correlate with C—C and C—O bond stretching. We use the absorbance ratio at 1047 cm^{-1} and 1022 cm^{-1} ($R_{1047/1022}$) to measure the short-range ordered conformation of the starch granules. The crystalline content of starch is indicated by the relative intensity of the peak at 1047 cm^{-1}. Meanwhile, the absorption peak at 1022 cm^{-1} denotes the amorphous structure. The higher value of $R_{1047/1022}$ indicates a higher degree of crystallization and ordered structure(Wang et al., 2021). The absorbance ratio at 995 cm^{-1} and 1022 cm^{-1} ($R_{995/1022}$) measures the degree of ordering of the double helices distributed inside the crystalline structure. The higher percentage of $R_{995/1022}$ indicates a higher degree of ordering of the double helix structure inside the starch. Starch undergoes pasting, disrupting the original starch structure and leading to short-range ordering changes (Table 3). $R_{1047/1022}$ and $R_{995/1022}$ decreased with the addition of EESDF. This was because EESDF disrupts the hydrogen bonding between water and starch molecules and the formation of starch lipid compounds. (Yu et al., 2018). In addition, EESDF was hydrophilic and reduced the motility of starch chains when the starch molecules were retrograded(Tang et al., 2013). $R_{1047/1022}$ and $R_{995/1022}$ increased from 0.7433 and 0.8291 to 0.8371 and 0.8754 during storage of native starch gels. This suggested that the rearrangement of amylopectin during long-term starch retrogradation resulted in gel stiffening and increased gel crystallinity and orderliness. The addition of EESDF retarded the recrystallization of starch, relatively increased the disordered structure, depleted the double helix structure, and inhibited the aggregation of starch during storage. The above findings demonstrated that EESDF retarded the retrogradation of CS during storage at 4 °C.

3.5. Effect of EESDF on the gel hardness of CS

Fig. 3 illustrates the effect of varying concentrations of EESDF on the hardness of starch gels. The starch molecules were reconnected into an ordered network structure during starch paste cooling. The starch gels were kept at 4 °C to promote starch retrogradation. The higher the extent of starch retrogradation, the stronger the structural ordering of the molecules, the stronger the bonding between starch molecules, the denser the starch gels formed, and the greater the gel hardness. The hardness of the starch gels grew markedly as the storage time increased. The gel hardness of CS storage at 1 d and 14 d was 258.14 g and 756.73 g, respectively. Studies have shown that short-term retrogradation of starch is associated with the ordered arrangement of amylose and long-term retrogradation is associated with the rearrangement of amylopectin.

Adding 1 % EESDF dramatically reduced the gel hardness of starch during storage to 228.80 g and 712.97 g at 1 d and 14 d, respectively. This indicated that EESDF interfered with the hydrogen bond formation

Table 3
Effects of EESDF on the short-range ordered structure of CS with different EESDF additions and in vitro starch digestion kinetics, estimated glycemic index, and hydrolysis index of CS with different additions of EESDF.

samples	storage time (day)	R1047/1022	R995/1022	C_∞(%)	K(10^{-2} , min^{-1})	HI	eGI
CS	0 d	0.7433 ± 0.005^{g}	0.8291 ± 0.002^{g}	83.92 ± 0.16^{a}	9.87 ± 1.35^{ab}	142.55	117.97
	14 d	0.8371 ± 0.001^{a}	0.8754 ± 0.007^{a}	82.18 ± 0.21^{b}	10.60 ± 1.57^{a}	140.17	116.66
CS-1 %EESDF	0 d	$0.7410 \pm 0.003^{i,j}$	0.8221 ± 0.002^{h}	82.72 ± 0.23^{b}	8.51 ± 1.13^{abc}	139.19	116.12
	14 d	0.8308 ± 0.002^{b}	0.8685 ± 0.002^{b}	79.01 ± 0.48^{d}	7.84 ± 1.18^{bcd}	132.14	112.26
CS-2 %EESDF	0 d	0.7422 ± 0.001^{h}	0.8178 ± 0.015^{i}	82.11 ± 0.63^{b}	8.42 ± 1.33^{abc}	138.06	115.50
	14 d	0.8259 ± 0.001^{d}	0.8632 ± 0.003^{d}	79.31 ± 0.01^{d}	7.82 ± 0.94^{bcd}	132.61	112.51
CS-3 %EESDF	0 d	0.7402 ± 0.004^{j}	0.7991 ± 0.002^{j}	81.93 ± 0.28^{b}	8.24 ± 1.12^{bc}	137.53	115.21
	14 d	0.8264 ± 0.002^{c}	0.8648 ± 0.005^{c}	79.47 ± 0.87^{cd}	7.62 ± 0.85^{cd}	132.62	112.52
CS-5 %EESDF	0 d	0.7401 ± 0.005^{j}	0.7852 ± 0.006^{k}	80.34 ± 0.14^{c}	7.91 ± 1.01^{bcd}	134.45	113.52
	14 d	0.8154 ± 0.005^{e8}	0.8510 ± 0.003^{e}	76.74 ± 0.43^{f}	5.76 ± 0.77^{de}	124.81	108.23
CS-10 %EESDF	0 d	0.7040 ± 0.003^{k}	0.7575 ± 0.003^{h}	77.85 ± 0.11^{e}	6.36 ± 0.76^{cde}	127.88	109.92
	14 d	0.8011 ± 0.007^{f}	0.8301 ± 0.007^{f}	70.58 ± 0.61^{g}	4.55 ± 0.65^{e}	111.52	100.94

Note: Different letters in the same column indicate significant differences ($p < 0.05$).

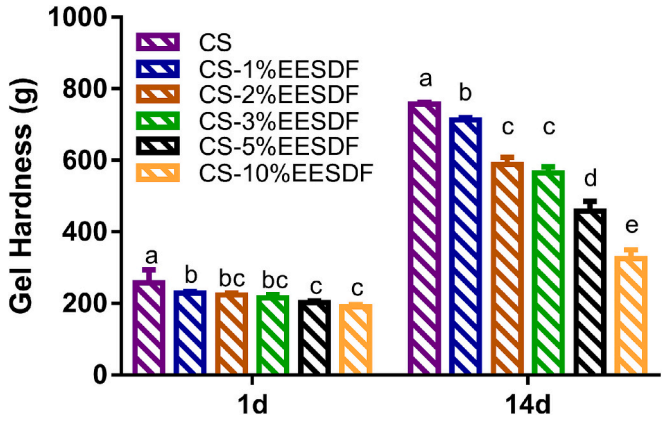

Fig. 3. Gel hardness of CS stored at 4 °C for 1 d and 14 d with different concentrations of EESDF.

during the recrystallization of amylopectin and amylose, affecting the starch's short-range and long-range ordered structures. This also indicated that EESDF interfered with the formation of the starch gel network, reducing the gel hardness. In all concentration ranges, the incorporation of 10 % EESDF had the most apparent effect on the reduction of starch gel hardness, reducing the hardness to 190.32 g and 325.56 g at 1 d and 14 d, respectively. Interestingly, we observed that the decline in gel hardness followed an approximately linear downward trend as the amount of EESDF increased. The results demonstrated that 10 % EESDF markedly inhibited starch retrogradation throughout the long- and short-term. This phenomenon was also found in the mixed system of soybean soluble polysaccharide, *Pueraria lobata* starch, and lotus root starch(Han et al., 2024). The interaction between water and hydrophilic colloids affected the starch network structure, thereby reducing the hardness of starch gels.

3.6. Effect of EESDF on the moisture distribution of CS gels

The distribution and migration of water during the pasting and retrogradation processes markedly influenced the properties of starch gels. LF-NMR is a useful method for detecting the water status and water-holding capacity of samples. The relaxation data from LF-NMR can show the two water states in the gel system.

The spin relaxation times (T_2) of CS gels with different proportions of EESDF at 0 d and 14 d are shown in Table 4. Fitting the low-field-strength resonance NMR data using a multi-exponential model shows four moisture characteristic peaks, and T_{2b}, T_{21}, T_{22}, and T_{23} demonstrate the four different spin relaxation times. Previous studies have shown that T_2 at < 1 ms is tightly bound and immobilized water, T_2 in the 1–30 ms range represented infirmly bound water, and the proton relaxation range of $T_2 > 100$ ms represented either cellular free water or cellular interstitial water(Belton, 1997). Therefore, in this test, T_{2b} represents bound water, T_{21}, and T_{22} are infirmly bound water, and T_{23} is interstitial-free water in the gel cells. Low field strength NMR can sense the degree of water fluctuation within the gel and, according to the degree of fluctuation, exhibits different T_2 values. The larger the T_2 value, the higher the degree of flexibility and mobility of the water molecules, which indicates that the water is loosely bound to the substrate. On the contrary, it represents that the water is tightly bound to the substrate. Bound water is the water molecules in the starch structure, weakly bound water is the water adsorbed on the surface of starch granules, and intercellular water represents the water in the network structure arranged by starch molecules. After adding EESDF, the relaxation time of tightly bound water, infirmly bound water, and intercellular water showed downward trends. This informed that adding EESDF enhanced the ability of starch molecules to bind water through enhanced hydrogen bonding interactions, as confirmed by the FTIR results. Zhao et al. (2021) found the same results in a mixed system of soluble soybean polysaccharides and four starches (corn starch, wheat starch, rice starch, and tapioca starch).

The excellent hydration capacity of EESDF helps starch gels retain more water. The decrease in the weakly bound water relaxation time

Table 4
Relaxation time of four types of moisture in CS gels with EESDF.

Samples	0 d Relaxation time (ms)				14 d Relaxation time (ms)			
	T_{2b}	T_{21}	T_{22}	T_{23}	T_{2b}	T_{21}	T_{22}	T_{23}
CS	0.87 ± 0.06^{a}	3.511 ± 0.09^{a}	12.328 ± 0.00^{a}	265.609 ± 0.00^{a}	0.107 ± 0.00^{b}	2.31 ± 0.02^{b}	10.723 ± 0.00^{a}	200.923 ± 0.00^{a}
CS-1 %EESDF	0.498 ± 0.06^{b}	1.748 ± 0.03^{d}	10.723 ± 0.00^{b}	265.609 ± 0.00^{a}	0.107 ± 0.00^{b}	2.656 ± 0.07^{a}	10.723 ± 0.00^{a}	200.923 ± 0.00^{a}
CS-2 %EESDF	0.327 ± 0.01^{c}	2.656 ± 0.02^{b}	12.328 ± 0.00^{a}	265.609 ± 0.00^{a}	0.163 ± 0.01^{a}	1.748 ± 0.00^{d}	8.111 ± 0.00^{c}	200.923 ± 0.00^{a}
CS-3 %EESDF	0.285 ± 0.01^{d}	2.009 ± 0.05^{c}	12.328 ± 0.00^{a}	265.609 ± 0.00^{a}	NM	2.009 ± 0.05^{c}	9.326 ± 0.06^{b}	200.923 ± 0.00^{a}
CS-5 %EESDF	0.142 ± 0.00^{e}	1.52 ± 0.07^{e}	10.723 ± 0.00^{b}	231.013 ± 5.16^{b}	NM	1.748 ± 0.00^{d}	8.111 ± 0.00c	174.753 ± 5.21^{b}
CS-10 %EESDF	0.142 ± 0.00^{e}	1.15 ± 0.01^{f}	9.326 ± 0.06^{c}	200.923 ± 1.86^{c}	NM	1.15 ± 0.01^{e}	9.326 ± 0.06^{b}	132.194 ± 0.00^{c}

Note: Different letters in the same column indicate significant differences($p < 0.05$). NM: not measured.

could be due to the binding ability of EESDF to water being stronger than that between starch and water. The T_{2b} signal disappeared when the starch gels were stored for 14 d. This was possibly due to structural changes in the starch during storage, which led to a decline in the water-tight binding region. Meanwhile, the T_2 value of 14 d appeared to have a downward trend compared with the T_2 value of 0 d. This was because of the dehydration that appeared during starch retrogradation, which changed the degree of water binding.

3.7. Effect of EESDF on the crystal structure of CS

X-ray diffraction is a typical method to evaluate the crystalline state of starch samples. Fig. S2 shows the X-ray diffraction types of CS gels stored at 4 °C for 1 d and 14 d. It was already documented that native CS displayed a typical A-type profile with diffraction peaks near 2θ of 15°, 17°, 18° and 23°. Fig. S2 (A) showed a typical B-type diffraction structure of CS gels, which demonstrated that the damage of starch granules during the gelatinization process destroyed the A-type structure. Then, the cooling of the starch paste led to the aggregation of amylose and amylopectin to arrange the B-type structure. As we all know, A-type crystals have short branched chains and loose double helices, while B-type crystals have a dense cluster-like branched structure. This difference in structure leads to different ways of being hydrolyzed by enzymes during digestion(Zhang et al., 2006). A-type starch undergoes internal hydrolysis first, whereas B-type starch undergoes external hydrolysis initially due to the absence of a pathway linking the outer layer and inner core of starch particles. Ma et al. (2024) suggested that the variance in the enzymatic hydrolysis pattern between the two starch crystals might affect the digestibility of the starch. Fig. S2 (B) shows the XRD patterns of starch gels stored after 14 d. Each curve had a diffraction peak at 2θ of 20°, representing a typical V-type structure. The formation of V-type structures is due to the interactions between lipids and amylose, which form a single-helix complex or the interaction between EESDF and starch(Yu et al., 2018).

The change in relative crystallinity (RC) of starch reflects the degree of ordered structure formation during starch retrogradation. The RC of gels with EESDF added to starch showed a decreasing trend. This is because hydrophilic colloids have good water solubility and are more readily dispersed in the starch-water mixture, which interferes with the hydrogen bonding of starch molecules and the generation of ordered structures. In addition, hydrophilic colloids can form copolymers with lipids and amylose, inhibiting starch recrystallization (Yang et al., 2010). The RC of CS gels increased from 5.36 % to 13.54 % during the storage period, indicating that the recrystallization of starch molecules during storage at 4 °C resulted in an increased ordering. The RC of CS was reduced after adding EESDF. 1 % EESDF reduced the RC of starch from 13.54 % to 12.82 % at 14 d. 10 % EESDF reduced the RC of starch from 13.54 % to 8.72 % at 14 d. These reductions were due to the interaction of EESDF with starch and water, thus interfering with the recrystallization of amylopectin. The reduction of RC showed that the addition of EESDF inhibited the long-term retrogradation of CS. This is similar to the results of DSC and FT-IR.

3.8. Effect of EESDF on the digestion properties of CS

The digestion properties of starch are firmly related to fluctuations in postprandial blood glucose and are important parameters. Understanding the digestion kinetics of starch can assist in developing dietary strategies to enhance glycemic management. It is essential for reducing the risk of type II diabetes(Bhupathiraju et al., 2014). Depending on the digestion rate, starches are categorized as rapidly digestible starch (RDS), slowly digestible starch (SDS), and resistant starch (RS). SDS and RS have slower digestion rates. RS is a type of starch that cannot be completely digested and absorbed. Table S1 illustrates the effect of modified soluble dietary fiber on the digestive properties of CS. Both stored at 4 °C for 0 d and 14 d, RDS content decreased, while SDS and RS contents increased with the addition of EESDF. When 10 % EESDF was added, the SDS content was the highest among all the groups. This may be because of the hydrogen bonding interaction between EESDF and the leached amylose, which resulted in unstable and loosely structured amylose polymers (Liu et al., 2019). This conclusion was also confirmed in FT-IR. The RS content increased as the addition of EESDF increased. This may be because the increased EESDF concentration content enhanced the physical barrier layer formed on the surface of the starch granules.(Zhuang et al., 2024) This enhancement inhibited the contact between the starch granules and the enzyme. These phenomena indicated that EESDF inhibited starch digestion in both long- and short-term retrogradation.

The effect of different concentrations of EESDF on the starch digestion curves is shown in Fig. 4. The trends of starch digestion curves for different storage times (0 d and 14 d) were similar, and the curves shifted downward after adding EESDF. It indicated that the starch digestibility decreased after the addition of EESDF. The downward shift of the starch digestion curve was more pronounced at 14 d compared with 0 d. The digestion rate of starch was markedly reduced. Incorporating 10 % EESDF reduced the rate of starch hydrolysis most notably. The increase in crystalline regions resulted in slow starch digestion.

Based on the starch digestion data, the equilibrium concentration C_∞(%)and kinetic constant K (10^{-2}, min^{-1}) obtained from the starch digestion curve fitting using a first-order kinetic model are shown in Table 3. The infinite digestion time of CS stored for 0 d and 14 d corresponded to starch digestion amount C_∞(%), and hydrolysis kinetic constant K showed a decreasing trend. The consequences indicated that the amount and rate of starch digestion decreased with the addition of EESDF. The amount of starch hydrolyzed showed the same trend as the digestion rate, suggesting a correlation between the amount of starch hydrolyzed and the rate of glucose release. The estimated glycemic index (eGI) of all the samples was distributed between 117.97 and 100.94, indicating that the composite starch gels were high-GI products, but it is obvious that the addition of EESDF decreased the eGI of CS to a certain extent. Adding 10 % EESDF at 0 d and 14 d storage decreased the eGI. This suggested that the EESDF decreased the rate and the extent of starch digestion during both short-term and long-term storage.

There are several hypotheses about the influence of dietary fiber on starch digestion properties: (1) Dietary fibers change the viscosity of starch food, thus changing the digestibility of starch. In the study of in vitro digestion of mushroom β-glucan and wheat systems, dietary fibers could be entangled with the starch chain, increasing the system's viscosity and decreasing the system's mobility(Zhuang et al., 2017). This was not favorable for amylase hydrolysis. (2) Dietary fibers with viscosity absorb water and form a thick solution that encapsulates the starch granules, reducing the contact of starch with enzyme hydrolysis, thus reducing starch digestibility. This was also found in the study of yellow mustard mucilage, soluble flaxseed gum, fenugreek gum, and oat gum with corn starch system by Repin et al. (2018). (3) Starch and dietary fibers interact to enhance the crystalline structure of starch retrogradation, and the ordered structure is not conducive to starch digestion. The texture-enhanced starch has a tightly ordered structure, which is unfavorable to the action of starch-digesting enzymes, thus reducing starch digestibility. (4)Dietary fibers inhibit amylase activity through physical adsorption or complexation, thereby reducing starch digestibility(Kong et al., 2020). This trend has also been found in barley β-glucan and corn starch mixed systems(Xiao et al., 2020) and jelly grass polysaccharide-cassava starch mixed systems(Zhang et al., 2019).

4. Conclusion

In this work, the effect of EESDF on the processing properties, retrogradation properties, and digestion properties of CS was investigated. The results showed that hydrogen bonding was the main interaction force between starch and EESDF. The incorporation of EESDF inhibited pasting, forming short-range and long-range ordered

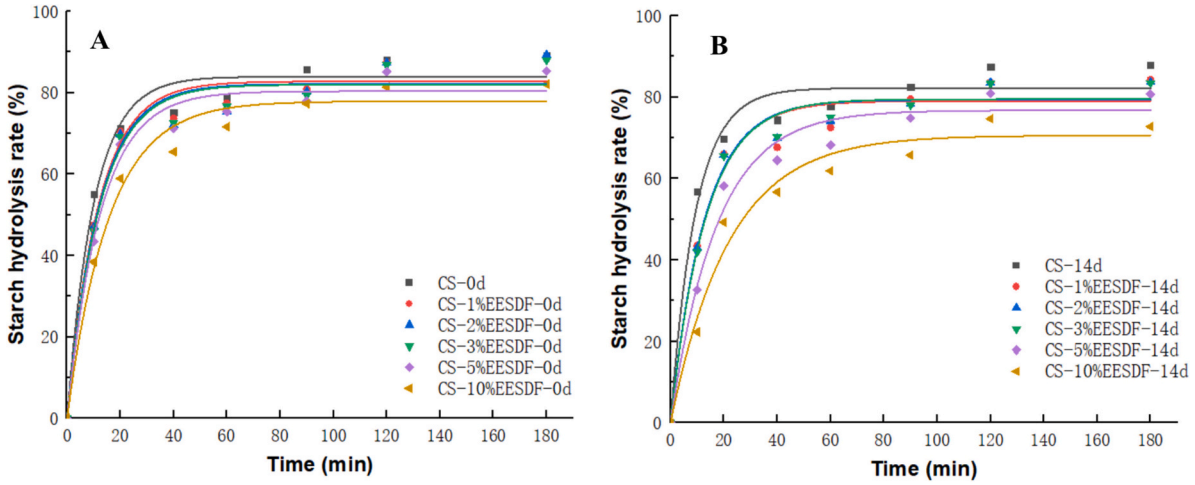

Fig. 4. Hydrolysis curves of corn starch gels stored at 4 °C for 0 d (A) and 14 d (B) with different EESDF additions.

structures, improved shear stability, and decreased the enthalpy of gelatinization, enthalpy of retrogradation, and gel hardness of starch. These results indicated that EESDF inhibited short-term and long-term retrogradation of CS. Furthermore, EESDF reduced the percentage of rapidly digestible starch, inhibited starch hydrolysis, and reduced the gluconeogenic index of starch. These findings provide insights into the interactions between starch and dietary fiber and the design of starch-based foods, promising applications in developing food products with enhanced nutritional benefits.

CRediT authorship contribution statement

Sheng Li: Writing – original draft, Supervision, Funding acquisition, Conceptualization. **Yuqian Zheng:** Software, Data curation. **Zhilong Chen:** Data curation. **Wenlong Xie:** Data curation. **Liping Xiao:** Software. **Dengji Gao:** Software. **Jun Zhao:** Supervision, Funding acquisition, Conceptualization.

Declaration of competing interest

The authors declare that they have no known competing financial interests or personal relationships that could have appeared to influence the work reported in this paper.

Acknowledgment

This work was supported by grants from the Climbing plan projects of Changchun University (ZKP202301), the Science and Technology Research Program of Education Department of Jilin Province of China (JJKH20240750KJ).

Appendix A. Supplementary data

Supplementary data to this article can be found online at https://doi.org/10.1016/j.fochx.2024.102013.

Data availability

Data will be made available on request.

References

Belton, P. S. (1997). NMR and the mobility of water in polysaccharide gels. *International Journal of Biological Macromolecules, 21*(1–2), 81–88. https://doi.org/10.1016/s0141-8130(97)00045-7

Bhupathiraju, S. N., Tobias, D. K., Malik, V. S., Pan, A., Hruby, A., Manson, J. E., & Hu, F. B. (2014). Glycemic index, glycemic load, and risk of type 2 diabetes: Results from 3 large US cohorts and an updated meta-analysis123. *The American Journal of Clinical Nutrition, 100*(1), 218–232. https://doi.org/10.3945/ajcn.113.079533

Englyst, H. N., Kingman, S. M., & Cummings, J. H. (1992). Classification and measurement of nutritionally important starch fractions. *European Journal of Clinical Nutrition, 46 Suppl 2*, S33–S50. ://MEDLINE:1330528.

Han, X., Liang, Q., Rashid, A., Qayum, A., Rehman, A., Zhong, M., & Ren, X. (2024). The effects of different hydrocolloids on lotus root starch gelatinization and gels properties. *International Journal of Biological Macromolecules, 257*, Article 128562. https://doi.org/10.1016/j.ijbiomac.2023.128562

Ji, X., Guo, J., Tian, J., Ma, K., & Liu, Y. (2023). Research progress on degradation methods and product properties of plant polysaccharides. *Journal of Light Industry, 38*(3), 55–62. https://doi.org/10.12187/2023.03.007

Joshi, M., Aldred, P., Panozzo, J. F., Kasapis, S., & Adhikari, B. (2014). Rheological and microstructural characteristics of lentil starch-lentil protein composite pastes and gels. *Food Hydrocolloids, 35*, 226–237. https://doi.org/10.1016/j.foodhyd.2013.05.016

Kong, X.-R., Zhu, Z.-Y., Zhang, X.-J., & Zhu, Y.-M. (2020). Effects of Cordyceps polysaccharides on pasting properties and in vitro starch digestibility of wheat starch. *Food Hydrocolloids, 102*, Article 105604. https://doi.org/10.1016/j.foodhyd.2019.105604

Lei, N., Chai, S., Xu, M., Ji, J., Mao, H., Yan, S., & Sun, B. (2020). Effect of dry heating treatment on multi-levels of structure and physicochemical properties of maize starch: A thermodynamic study. *International Journal of Biological Macromolecules, 147*, 109–116. https://doi.org/10.1016/j.ijbiomac.2020.01.060

Li, M., Li, L., Sun, B., & Ma, S. (2024). Interaction of wheat bran dietary fiber-gluten protein affects dough product: A critical review. *International Journal of Biological Macromolecules, 255*, Article 128199. https://doi.org/10.1016/j.ijbiomac.2023.128199

Li, M., & Ma, S. (2024). A review of healthy role of dietary fiber in modulating chronic diseases. *Food Research International*. https://doi.org/10.1016/j.foodres.2024.114682

Li, S., Hu, N., Zhu, J., Zheng, M., Liu, H., & Liu, J. (2022). Influence of modification methods on physicochemical and structural properties of soluble dietary fiber from corn bran. *Food Chemistry: X, 14*, Article 100298. https://doi.org/10.1016/j.fochx.2022.100298

Liu, C., Zhang, H., Chen, R., Chen, J., Liu, X., Luo, S., & Chen, T. (2021). Effects of creeping fig seed polysaccharide on pasting, rheological, textural properties and in vitro digestibility of potato starch. *Food Hydrocolloids, 118*. https://doi.org/10.1016/j.foodhyd.2021.106810

Liu, X., Liu, S., Xi, H., Xu, J., Deng, D., & Huang, G. (2019). Effects of soluble dietary fiber on the crystallinity, pasting, rheological, and morphological properties of corn resistant starch. *LWT, 111*, 632–639. https://doi.org/10.1016/j.lwt.2019.01.059

Lu, L., He, C., Liu, B., Wen, Q., & Xia, S. (2022). Incorporation of chickpea flour into biscuits improves the physicochemical properties and in vitro starch digestibility. *Lwt-Food Science and Technology, 159*. https://doi.org/10.1016/j.lwt.2022.113222

Luo, D., Li, Y., Xu, B., Ren, G., Li, P., Li, X., & Liu, J. (2017). Effects of inulin with different degree of polymerization on gelatinization and retrogradation of wheat starch. *Food Chemistry, 229*, 35–43. https://doi.org/10.1016/j.foodchem.2017.02.058

Ma, Q., Wang, X., Appels, R., Zhang, D., Zhang, X., Zou, L., & Hu, X. (2024). Large flour aggregates containing ordered B+V starch crystals significantly improved the digestion resistance of starch in pretreated multigrain flour. *International Journal of Biological Macromolecules, 264*(Pt 2), 130719. https://doi.org/10.1016/j.ijbiomac.2024.130719

Ma, S., Wang, Z., Liu, H., Li, L., Zheng, X., Tian, X., & Wang, X. (2022). Supplementation of wheat flour products with wheat bran dietary fiber: Purpose, mechanisms, and

challenges. *Trends in Food Science & Technology*. https://doi.org/10.1016/j.tifs.2022.03.012

Pak, S., Chen, F., Ma, L., Hu, X., & Ji, J. (2021). Functional perspective of black fungi (Auricularia auricula): Major bioactive components, health benefits and potential mechanisms. *Trends in Food Science & Technology, 114*, 245–261. https://doi.org/10.1016/j.tifs.2021.05.013

Qiu, S., Yadav, M. P., Chen, H., Liu, Y., Tatsumi, E., & Yin, L. (2015). Effects of corn fiber gum (CFG) on the pasting and thermal behaviors of maize starch. *Carbohydrate Polymers, 115*, 246–252. https://doi.org/10.1016/j.carbpol.2014.08.071

Repin, N., Cui, S. W., & Goff, H. D. (2018). Impact of dietary fibre on in vitro digestibility of modified tapioca starch: Viscosity effect. *Bioactive Carbohydrates and Dietary Fibre, 15*, 2–11. https://doi.org/10.1016/j.bcdf.2016.11.002

Tang, M., Hong, Y., Gu, Z., Zhang, Y., & Cai, X. (2013). *The effect of xanthan on short and long-term retrogradation of rice starch.* Starch -. Strke.

Tester, R. F., & Sommerville, M. D. (2003). The effects of non-starch polysaccharides on the extent of gelatinisation, swelling and α-amylase hydrolysis of maize and wheat starches. *Food Hydrocolloids, 17*(1), 41–54. https://doi.org/10.1016/s0268-005x(02)00032-2

Tian, Y., Xu, X., Li, Y., Jin, Z., Chen, H., & Wang, H. (2009). Effect of β-cyclodextrin on the long-term retrogradation of rice starch. *European Food Research and Technology, 228*(5), 743–748. https://doi.org/10.1007/s00217-008-0985-9

Wang, N., Wu, L., Huang, S., Zhang, Y., Zhang, F., & Zheng, J. (2021). Combination treatment of bamboo shoot dietary fiber and dynamic high-pressure microfluidization on rice starch: Influence on physicochemical, structural, and in vitro digestion properties. *Food Chemistry, 350*. https://doi.org/10.1016/j.foodchem.2020.128724

Wang, N., Wu, L., Zhang, F., Kan, J., & Zheng, J. (2022). Modifying the rheological properties, in vitro digestion, and structure of rice starch by extrusion assisted addition with bamboo shoot dietary fiber. *Food Chemistry, 375*. https://doi.org/10.1016/j.foodchem.2021.131900

Wu, B., Degner, B., & McClements, D. J. (2013). Microstructure & rheology of mixed colloidal dispersions: Influence of pH-induced droplet aggregation on starch granule-fat droplet mixtures. *Journal of Food Engineering, 116*(2), 462–471. https://doi.org/10.1016/j.jfoodeng.2012.12.020

Xiao, Y., Liu, S., Shen, M., Jiang, L., Ren, Y., Luo, Y., & Xie, J. (2020). Effect of different Mesona chinensis polysaccharides on pasting, gelation, structural properties and in vitro digestibility of tapioca starch-Mesona chinensis polysaccharides gels. *Food Hydrocolloids, 99*. https://doi.org/10.1016/j.foodhyd.2019.105327

Xie, F., Zhang, H., Xia, Y., & Ai, L. (2020). Effects of tamarind seed polysaccharide on gelatinization, rheological, and structural properties of corn starch with different amylose/amylopectin ratios. *Food Hydrocolloids, 105*. https://doi.org/10.1016/j.foodhyd.2020.105854

Xu, N., Yu, P., Zhang, H., Ji, X., Wu, P., Zhang, L., & Wang, X. (2024). Effects of Laminaria japonica polysaccharide and coumaric acid on pasting, rheological, retrogradation and structural properties of corn starch. *International Journal of Biological Macromolecules, 263*. https://doi.org/10.1016/j.ijbiomac.2024.130343

Yang, Y., Gu, Z., Xu, H., Li, F., & Zhang, G. (2010). Interaction between amylose and β-Cyclodextrin investigated by complexing with conjugated linoleic acid. *Journal of Agricultural and Food Chemistry, 58*(9), 5620–5624. https://doi.org/10.1021/jf9043869

Ye, J., Hu, X., Luo, S., McClements, D. J., Liang, L., & Liu, C. (2018). Effect of endogenous proteins and lipids on starch digestibility in rice flour. *Food Research International, 106*, 404–409. https://doi.org/10.1016/j.foodres.2018.01.008

Yu, Z., Wang, Y.-S., Chen, H.-H., Li, Q.-Q., & Wang, Q. (2018). The gelatinization and retrogradation properties of wheat starch with the addition of stearic acid and sodium alginate. *Food Hydrocolloids, 81*, 77–86. https://doi.org/10.1016/j.foodhyd.2018.02.041

Zhang, G., Ao, Z., & Hamaker, B. R. (2006). Slow digestion property of native cereal starches. *Biomacromolecules, 7*(11), 3252–3258. https://doi.org/10.1021/bm060342i

Zhang, H., Li, Z., Tian, Y., Song, Z., & Ai, L. (2019). Interaction between barley β-glucan and corn starch and its effects on the in vitro digestion of starch. *International Journal of Biological Macromolecules, 141*, 240–246. https://doi.org/10.1016/j.ijbiomac.2019.08.268

Zhao, Q., Tian, H., Chen, L., Zeng, M., Qin, F., Wang, Z., & Chen, J. (2021). Interactions between soluble soybean polysaccharide and starch during the gelatinization and retrogradation: Effects of selected starch varieties. *Food Hydrocolloids, 118*. https://doi.org/10.1016/j.foodhyd.2021.106765

Zhong, Y., Xiang, X., Chen, T., Zou, P., Liu, Y., Ye, J., & Liu, C. (2020). Accelerated aging of rice by controlled microwave treatment. *Food Chemistry, 323*. https://doi.org/10.1016/j.foodchem.2020.126853

Zhou, D., Ma, Z., Yin, X., Hu, X., & Boye, J. I. (2019). Structural characteristics and physicochemical properties of field pea starch modified by physical, enzymatic, and acid treatments. *Food Hydrocolloids, 93*, 386–394. https://doi.org/10.1016/j.foodhyd.2019.02.048

Zhou, J., Jia, Z., Wang, M., Wang, Q., Barba, F. J., Wan, L., & Fu, Y. (2022). Effects of Laminaria japonica polysaccharides on gelatinization properties and long-term retrogradation of wheat starch. *Food Hydrocolloids, 133*. https://doi.org/10.1016/j.foodhyd.2022.107908

Zhuang, H., Chen, Z., Feng, T., Yang, Y., Zhang, J., Liu, G., & Ye, R. (2017). Characterization of Lentinus edodes β-glucan influencing the in vitro starch digestibility of wheat starch gel. *Food Chemistry, 224*, 294–301. https://doi.org/10.1016/j.foodchem.2016.12.087

Zhuang, J., Zhu, J., Cheung, P. C. K., & Li, C. (2024). The physical and chemical interactions between starch and dietary fiber: Their impact on the physicochemical and nutritional properties of starch. *Trends in Food Science & Technology, 149*, Article 104566. https://doi.org/10.1016/j.tifs.2024.104566